ASPECTS OF MODELING SOOT FORMATION IN TURBULENT DIFFUSION FLAMES

FABIAN MAUSS∗, [a] , KARL NETZELL [a] & HARRY
LEHTINIEMI [a]

[a] Division of Combustion Physics, Lund University,
Sweden
Version of record first published: 21 Sep 2006.

PLEASE SCROLL DOWN FOR ARTICLE

whatsoever or howsoever caused arising directly or indirectly in connection with or arising out of the use of this material.

Taylor & Francis
Taylor & Francis Group

ASPECTS OF MODELING SOOT FORMATION IN TURBULENT DIFFUSION FLAMES

FABIAN MAUSS*,†
KARL NETZELL
HARRY LEHTINIEMI

Division of Combustion Physics,
Lund University, Sweden

Soot formation in a turbulent jet diffusion flame is modeled using an unsteady flamelet approach. In the present work, we study the effects of the choice of the dependence of scalar dissipation rate on mixture fraction and agglomeration processes on the predicted soot volume fraction. It is found that good predictions of soot volume fraction can be obtained without considering preferential diffusion effects.

Keywords: interactive flamelets, soot formation, turbulent diffusion flame

INTRODUCTION

The formation of soot in turbulent diffusion flames is a problem in combustion that is still not understood. In the past, there have been two approaches to model this process using the laminar flamelet concept. The first approach was based on a flamelet library concept (Balthasar et al., 1996; Bai et al., 1998). In this approach a flamelet library for

the source terms of soot formation was generated. A transport equation for the soot volume fraction, that used the source terms from the library, was included in the CFD calculation. The second approach was based on instationary flamelet calculations, which were either done in interaction with the CFD calculation, or have been done in a post-process (Mauss et al., 1990; Pitsch et al., 1998; Barths et al., 1998, 2000).

The flamelet library based method has the advantage of very low computational cost when coupled with a computational fluid dynamics code as the method requires only the transport of two additional scalars, the mixture fraction and the mixture fraction variance. The interactive flamelet method has the advantage of not only including transient effects occurring in the soot formation processes, but also in the combustion process itself. Transient effects in the profiles of important intermediate species, such as radicals and soot precursors, may have a significant impact on the source terms of particle inception, surface growth or oxidation. Therefore in this work, the representative interactive flamelet approach is chosen.

In a previous attempt to model soot formation in turbulent diffusion flames (Pitsch et al., 2000), it was concluded that in order to accurately predict soot volume fraction profiles, preferential diffusion for the soot particles has to be considered. In this work, we have chosen to use the unity Lewis number simplification, in order to study the effects of other parameters. Here we investigate the choice of the dependence of scalar dissipation rate on mixture fraction and the influence of agglomeration processes. The ethylene flame experiments by Young et al. (1991) provide the data for this study. They have been used recently by Ma et al. (2005) to validate an empirical soot model. The model used for soot prediction in the present work is a detailed kinetic model.

THE DETAILED KINETIC SOOT MODEL

The detailed kinetic soot model follows the approach by Mauss (1998). A sketch of the model is given in Figure 1. During the oxidation of the hydrocarbon fuel, aromatic species are formed in the gas phase of the flame and grow to poly-aromatic structures. Species with more than four rings can combine and incept soot particles (Schuetz and Frenklach, 2002). They can further condense on the soot particle surface and contribute to the surface growth process. Soot particles collide and, depending on their size and the surrounding environment, combine to larger spherical particles or to agglomerates (Mitchell and Frenklach,
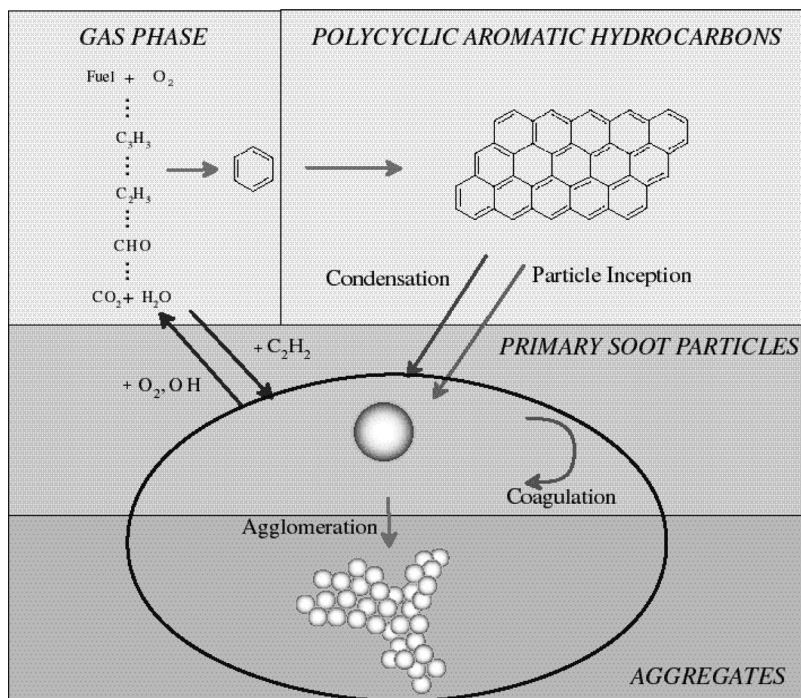
Figure 1. A sketch of the detailed kinetic soot model.

2003). All these processes can be calculated from the Smoluchowski equation. In addition heterogeneous surface growth and oxidation reactions are taken into account. The surface growth is modeled by the simple hydrogen abstraction acetylene addition mechanism (HACA) (Frenklach and Wang, 1990). Oxidation occurs via reactions of OH and O_2 on the soot particle surface. Details of the soot model are not part of this work, and can be found in Mauss (1998). In addition to that model, the agglomeration model by Kazakov and Frenklach (1998) was added. For the reference calculation the fractal dimension of the particles was kept constant $D_f = 1.8$.

The soot model introduces an infinite number of partial differential equations that describe the particle size distribution function. It is not possible to solve this system of equations for one-dimensional flame calculations, and it is necessary to model the particle size distribution function. Two mathematical methods are known from the literature, the method of moments (Frenklach and Wang, 1990) and the sectional

method (see Gelbard et al., 1990). Further methods do not allow the calculation of convective transport, or particle diffusion and are not taken into consideration here. In this work we use the method of moments to solve the particle size distribution function. This method is based on that any mathematical function can be described by its statistical moments. For the soot particle size distribution function, the moments are defined as:

$$M_r = \sum_{i=1}^{\infty} i^r N_i \tag{1}$$

The moment M_0 is the total number density of particles.

$$M_0 = \sum_{i=1}^{\infty} N_i = N \tag{2}$$

The moment M_1 holds the information about the particle mass fraction f_m, or the particle volume fraction f_v.

$$M_1 = \sum_{i=1}^{\infty} i N_i = f_v \frac{\rho_s}{m_1} \tag{3}$$

The moment M_2 can be used to calculate the variance of the particle size distribution function, while the moment M_3 holds information about the skewness of this function. The variance is thus given by:

$$\sigma^2 = \frac{M_2}{M_0} - \left(\frac{M_1}{M_0}\right)^2 \tag{4}$$

The number of transported moments determines the accuracy of the description of the particle size distribution function. Further details on the method of moments can be found in Frenklach (2002).

INSTATIONARY FLAMELET MODELING

Soot formation in turbulent diffusion flames was recently investigated by Pitsch et al. (2000). In this publication it was concluded that it is necessary to include preferential diffusion effects for soot particles, to be able to predict the measured profiles for the soot volume fraction in a turbulent ethylene-air jet diffusion flame. Since we found that the predicted profile for the soot volume fraction is very sensitive on a number of parameters, it is necessary to present some of the details of the modeling approach.

The set of one-dimensional equations in the mixture fraction coordinate can be derived by transforming the set of three-dimensional

equations in space (see Pitsch and Peters, 1998). The following formulation for the conservation of species and energy is equivalent to the formulation in their work. The formulation of the transport of species number density Fick's law for the diffusion of particles has been applied, as before in Mauss (1998) and Mauss et al. (1994).

Conservation of species

$$\rho \frac{dY_i}{dt} = \frac{\rho\chi}{2}\frac{dF_i}{dZ} + \frac{G_i}{4} + \dot{\omega}_i \tag{5}$$

with

$$F_i = \frac{Y_i}{Le_i X_i}\frac{dX_i}{dZ} - Y_i \sum_{k=1}^{N}\left(\frac{Y_k}{Le_k X_k}\frac{dX_k}{dZ}\right)$$

$$G_i = \left(F_i - \frac{dY_i}{dZ}\right)\left(\frac{d}{dZ}(\rho\chi) + \frac{\chi}{D}\frac{d}{dZ}(\rho D)\right) \tag{6}$$

Conservation of soot particle number density

$$\rho \frac{d\overline{N}_i}{dt} = \frac{\rho\chi}{2}\frac{dF_i^*}{dZ} + \frac{G_i^*}{4} + \dot{\omega}_i$$

$$\overline{N}_i = \frac{N_i}{\rho N_A} \tag{7}$$

with

$$F_i^* = \frac{1}{Le_i}\frac{d\overline{N}_i}{dZ}$$

$$G_i^* = \left(F_i^* - \frac{d\overline{N}_i}{dZ}\right)\left(\frac{d}{dZ}(\rho\chi) + \frac{\chi}{D}\frac{d}{dZ}(\rho D)\right) \tag{8}$$

Conservation of energy

$$\rho c_p \frac{dT}{dt} = \frac{\rho\chi}{2}\left(\frac{d}{dZ}\left(c_p\frac{dT}{dZ}\right) + H\right) - \sum_{i=1}^{N} h_i\omega_i - q_R \tag{9}$$

with

$$H = \sum_{i=1}^{N}(c_{p,i}F_i)\frac{dT}{dZ}$$

$$q_R = \sum_{i=1}^{N}\alpha_i\sigma(T^4 - T_0^4) \tag{10}$$

The Lewis number for the particles in Eq. (8) can be expressed in terms of the Lewis number of the smallest particle size, and the number of monomers in the particle.

$$Le_i = Le_0 j^{(2/3)} \tag{11}$$

Using the definition of the moments for the particle size distribution function (1), the transport equation for the number densities of the particle size distribution function (7) can be transformed into the transport equation for the moments of the particle size distribution function.

$$\rho \frac{d\overline{M}_r}{dt} = \frac{\rho\chi}{2}\frac{dF_r}{dZ} + \frac{G_r}{4} + \dot{\omega}_r$$
$$\overline{M}_r = \frac{M_r}{\rho N_A} \tag{12}$$

with:

$$F_r = \frac{1}{Le_0}\frac{d\overline{M}_{r-2/3}}{dZ}$$
$$G_r = \left(F_r - \frac{d\overline{M}_r}{dZ}\right)\left(\frac{d}{dZ}(\rho\chi) + \frac{\chi}{D}\frac{d}{dZ}(\rho D)\right) \tag{13}$$

It is worthwhile to notice that $F_r = 0$, in case of very large soot particles. However this assumption has also other consequences, which will not be discussed further here.

Under the assumption that the Lewis number is equal to unity this set of equations is simplified significantly:

$$F_i = \frac{dY_i}{dZ}; \quad F_i^* = \frac{d\overline{N}_i}{dZ}; \quad G = 0 \tag{14}$$

The assumption of unity Lewis numbers are frequently used in the literature and the conservation equations can be given as follows:

Conservation of species

$$\rho\frac{dY_i}{dt} = \frac{\rho\chi}{2}\frac{d^2 Y_i}{dZ^2} + \dot{\omega}_i \tag{15}$$

Conservation of soot number densities:

$$\rho\frac{d\overline{N}_i}{dt} = \frac{\rho\chi}{2}\frac{d^2\overline{N}_i}{dZ^2} + \dot{\omega}_i \tag{16}$$

Conservation of energy:

$$\rho c_p \frac{dT}{dt} = \frac{\rho\chi}{2}\left(\frac{d}{dZ}\left(c_p\frac{dT}{dZ}\right) + \sum_{i=1}^{N} c_{p,i}\frac{dY_i}{dZ}\frac{dT}{dZ}\right) - \sum_{i=1}^{N} h_i\omega_i - q_R \quad (17)$$

Finally the transport equation for the number densities of the soot particle size distribution function can be transformed into the transport equation for the moments of the particle size distribution function.

$$\rho\frac{d\overline{M}_r}{dt} = \frac{\rho\chi}{2}\frac{d^2\overline{M}_r}{dZ^2} + \dot{\omega}_r \quad (18)$$

The scalar dissipation rate χ in Eq. (18) is calculated from the conditional mean scalar dissipation rate at the position of maximum scalar dissipation in Z. This definition allows calculating the instationary flamelet at heights, where the maximum mixture fraction is smaller than the stoichiometric mixture fraction. The conditional mean scalar dissipation rate is calculated as suggested in Pitsch et al. (1998). We describe the dependence of the scalar dissipation on the mixture fraction Z using an inverse complementary error function that is defined between $Z = 0$ and $Z = Z_{max}$. We chose Z_{max} to be the mean of the mixture fraction on the centerline of the turbulent diffusion flame.

THE EXPERIMENTAL TEST FLAME

As in our previous work (Bai et al., 1998) we use the experiments by Young et al. (1991) on a rim-stabilized ethylene turbulent jet diffusion flame. Ethylene is injected through a pipe with a diameter of 3.1 mm at a speed of 24.5 m/s into stagnant air at room temperature and atmospheric pressure. The soot volume fraction was measured by laser absorption along with mixture fraction by microprobe sampling technique, and temperature by fine wire thermocouples.

THE REFERENCE CALCULATION USING THE INSTATIONARY FLAMELET MODEL

This section describes the results gained by using the instationary flamelet model. We use the set of equations (15, 17, 18), assuming that the Lewis number for all species are equal to unity. Only the influence of transient effects on the rates of soot formation is discussed herein.

Table 1. The heterogeneous surface reactions and their rate coefficients

Reaction	A [Mole, cm, sec, K]	n	E [kJ/mole]
$C_{S,i}H + H \longleftrightarrow C^*_{S,i} + H_2$	1.0E + 14	0.0	0.0
$C_{S,i}H + OH \longleftrightarrow C^*_{S,i} + H_2O$	1.6E + 08	1.4	6.1
$C^*_{S,i} + H \longleftrightarrow C_{S,i}H$	1.0E + 13	0.0	0.0
$C^*_{S,i} + C_2H_2 \longleftrightarrow C^*_{S,i}C_2H_2 + H_2$	3.5E + 13	0.0	0.0
$C^*_{S,i}C_2H_2 \longleftrightarrow C_{S,i+2}H + H$	1.0E + 10	0.0	20.0
$C^*_{S,i} + O_2 \longleftrightarrow C^*_{S,i-2} + 2CO$	1.0E + 12	0.0	8.4
$C^*_{S,i+2}C_2H_2 + O_2 \longleftrightarrow C^*_{S,i} + 2HCO$	1.0E + 12	0.0	8.4
$C_{S,i}H + OH \longleftrightarrow C^*_{S,i-2} + CH + HCO$	3.5E + 12	0.0	46.0

Details on the mixture fraction and flow velocity calculations have been reported previously (see Bai et al., 1998).

The reaction mechanism for the gas phase is identical to the mechanism used by Mauss (1998). The heterogeneous surface reaction mechanism was also taken from that work. However the rate coefficients were slightly changed as given in Table 1. The major difference is the reduction of the reaction rate coefficients for the oxidation reactions, which were set to 1.0E + 13 before. The oxidation reactions are more sensitive in diffusion flames, which are under consideration here, than in premixed flames that were under consideration in Mauss (1998). Furthermore agglomeration is considered following the approach by Kazakov and Frenklach (1998). The fractal dimension of the soot particles was assumed to be independent of the particle size and was kept constant and set to $D_f = 1.8$. This value has been found in experiments.

RESULTS AND DISCUSSION

The calculated axial temperature profile at the centerline is shown in Figure 2. It can be seen that the calculated temperature in the core of the flame is up to 200 K higher than found in the experiment. The mixture fraction becomes stoichiometric at a height of 350 mm. From this height the calculated temperature profile is in agreement with the experiments. The same can be concluded for the comparison between numerical calculation and the experiment of the radial temperature profile shown in Figure 3. At a height of 160 mm is the predicted temperature in the core of the flame about 200 K higher than the experimental. Calculation and prediction agree for stoichiometric and fuel
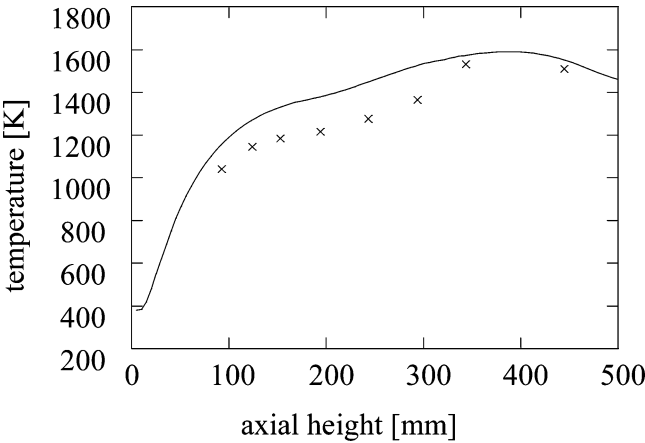
Figure 2. The axial temperature profile. The figure shows the numerically calculated profile (solid line) and the experiments by Young et al. (crosses). The dashed line indicates soot volume fraction for a calculation not considering maximum mixture fraction.

lean conditions. The results calculated from instationary flamelets are consistent with the results obtained by Bai et al. (1998), where a flamelet library was used. It is worthwhile to mention that temperature measurements with thermocouples in the core of a sooting turbulent diffusion
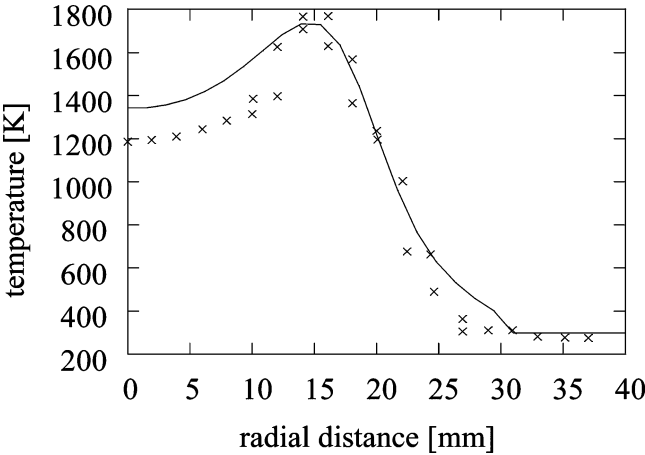

Figure 3. The radial temperature profile at a height of 160 mm. The figure shows the calculated profile (solid line) and the experiments by Young et al. (crosses).
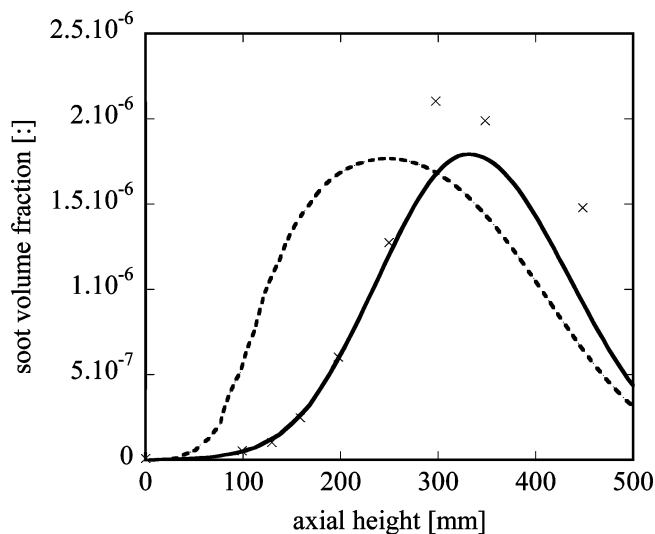
Figure 4. The axial profile of the soot volume fraction. The figure shows the numerically calculated profile (solid line) and the experiments by Young et al. (crosses).

flame are difficult to perform. The numerically calculated profiles for the soot volume fraction are compared with the experimental data in Figures 4–7. The axial profile of soot volume fraction can be seen in Figure 4, along with experimental data and a dashed line indicating soot volume
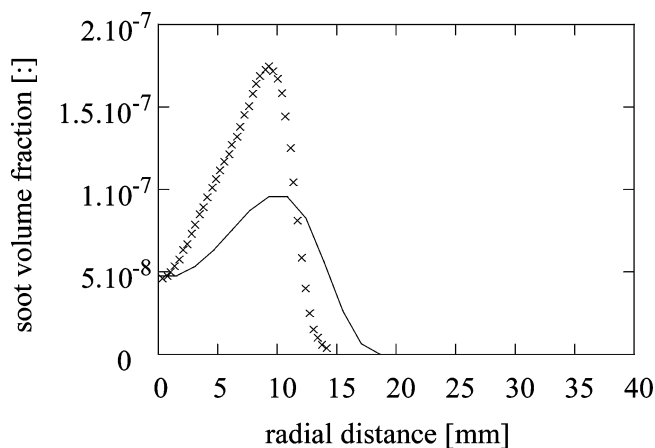
Figure 5. The radial profile of the soot volume fraction at a height of 100 mm.
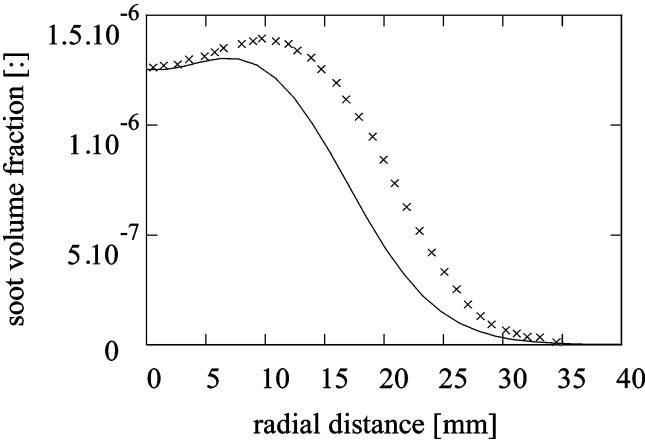
Figure 6. The radial profile of the soot volume fraction at a height of 250 mm.

fraction for a calculation not considering maximum mixture fraction. The shape and the height of the predicted profile in Figure 4 agree well with the experimental data. The maximum in the predicted soot volume fraction is lower than in the experimental data. This is most probably caused by an inaccuracy in the predicted mixture fraction field. The mixing occurs in the simulation faster than in the experiment. This can also be seen in Figures 6 and 7. It appears that the shape of the predicted
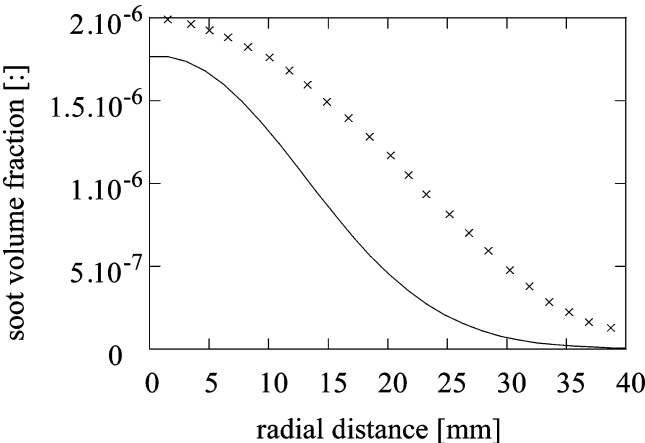

Figure 7. The radial profile of the soot volume fraction at a height of 350 mm.

and experimental profiles agree well. However, the numerical profiles are narrower.

The computed and experimentally determined axial mixture fraction profiles are shown in Figure 8, and the radial mixture fraction profile at a height of 160 mm is shown in Figure 9. It is observed that the axial mixture fraction is slightly underpredicted at low heights. In Figure 10, the effects of assuming simpler surface models are shown. Assuming all particles to be spherical makes the soot volume too low, and assuming all particles form chainlike structures of the smallest particles makes soot volume much too high. The approach of a constant fractal dimension as applied in this paper is simple, and more advanced agglomeration models for diffusion flames could improve the predictability of kinetic soot models.

Different from results by Pitsch et al. (2000), a good agreement between calculation and experiment could be found, without assuming preferential diffusion of soot. We found that there is a permanent loss of soot in the instationary flamelet model, if the decrease of the maximum mixture fraction, needed in the formulation of the scalar dissipation rate is not taken into account. The inclusion of the maximum
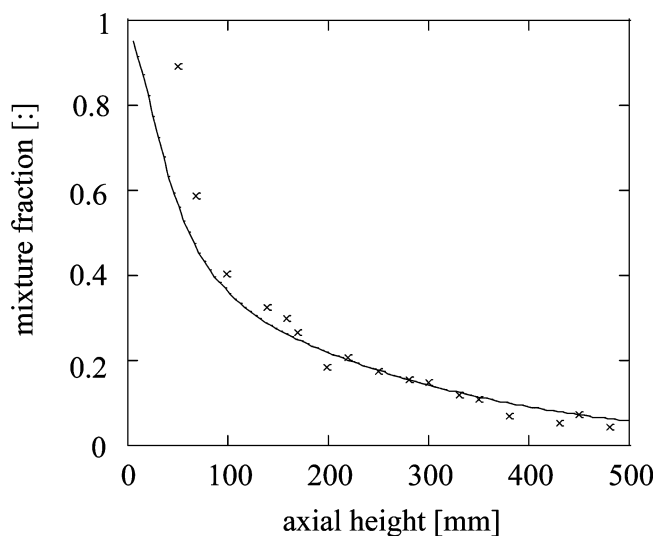

Figure 8. The axial mixture fraction profile. The computed mixture fraction profile (solid line) and the measured mixture fraction (crosses) are shown.
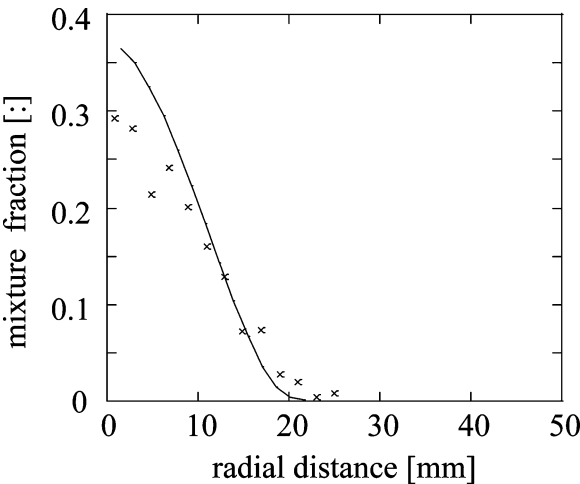
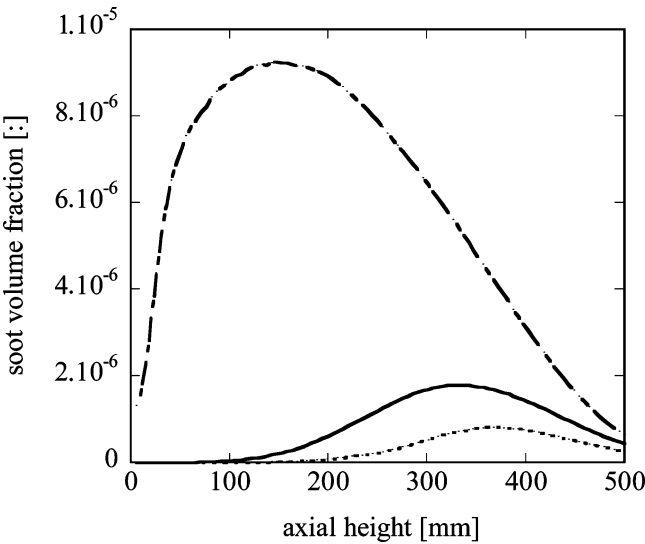**Figure 9.** The radial mixture fraction profile at a height of 160 mm.

Figure 10. The axial profile of the soot volume fraction. The figure shows the numerically calculated profile (solid line) and assuming spherical particles (short-dashed line) and assuming particles from chain of the small spherical particles (long-dashed line).

mixture fraction Z_{max} causes that the scalar dissipation rate becomes zero at $Z = Z_{max}$, causing that the diffusive terms in the flamelet equations become zero for $Z = Z_{max}$.

CONCLUSION

Soot formation in a turbulent ethylene diffusion flame was calculated using the instationary flamelet concept. A detailed chemical mechanism and a complex soot model were used. In this work, the impact of the scalar dissipation rate model in mixture fraction space and an agglomeration model on the predicted soot volume fraction was studied. The scalar dissipation rate was conditioned on the position in mixture fraction space on which maximum scalar dissipation rate occurs. The maximum mixture fraction was defined as the mixture fraction on the centerline. This method gives the possibility to define scalar dissipation rate and calculate instationary flamelets on heights, where the maximum mixture fraction is less than the stoichiometric mixture fraction. Furthermore, an agglomeration model was included. It was however assumed, in the calculations presented herein, that the fractal dimension of the soot particles is constant.

Using the approach presented here to model the dependence of scalar dissipation rate on mixture fraction, and by applying an agglomeration model, we found that a good prediction of the soot volume fraction profiles can be obtained without considering preferential diffusion effects.

REFERENCES

Bai, X.S., Fuchs, L., Balthasar, M., and Mauss, F. (1998) Detailed soot modelling in turbulent jet diffusion flames. *Proc. Combust. Instit.*, **27**, 1623–1630.

Balthasar, M., Heyl, A., Mauss, F., Schmitt, F., and Bockhorn, H. (1996) Flamelet modelling of soot in laminar ethyne/air diffusion flames. *Proc. Combust. Instit.*, **26**, 2369–2377.

Barths, H., Hasse, C., Bikas, G., and Peters, N. (2000) Simulation of combustion in direct injection diesel engines using a Eulerian particle flamelet model. *Proc. Combust. Instit.*, **28**, 1161–1168.

Barths, H., Peters, N., Brehm, N., Mack, A., Pfitzner, M., and Smiljanovski, V. (1998) Simulation of pollutant formation in a gas-turbine combustor using unsteady flamelets. *Proc. Combust. Instit.*, **27**, 1841–1847.

Frenklach, M. (2002) Method of moments with interpolative closure. *Chem. Eng. Sci.*, **57**, 2229–2239.

Frenklach, M. and Wang, H. (1990) Detailed modeling of soot particle nucleation and growth. *Proc. Combust. Instit.*, **23**, 1559–1566.

Gelbard, F., Tambour, Y., and Seinfeld, J.H. (1980) Sectional representations for simulating aerosol dynamics. *Journal Coll. Interface. Sci.*, **76**(2), 541–556.

Kazakov, A. and Frenklach, M. (1998) Dynamic modeling of soot particle coagulation and aggregation: implementation with the method of moments and application to high-pressure laminar premixed flames. *Combust. Flame*, **114**, 484–501.

Ma, G., Wen, J.Z., Lightstone, M.F., and Thomson, M.J. (2005) Optimization of soot modeling in turbulent nonpremixed ethylene/air jet flames. *Combust. Sci. Tech.*, **177**, 1567–1602.

Mauss, F. (1998) Entwicklung eines kinetischen Modells der Rußbildung mit schneller Polymerisation, D 82 (RWTH Aachen), ISBN 3-89712-152-2.

Mauss, F., Keller, D., and Peters, N. (1990) A lagrangian simulation of flamelet extinction and re-ignition in turbulent jet diffusion flames. *Proc. Combust. Instit.*, **23**, 693–698.

Mauss, F., Trilken, B., Breitbach, H., and Peters, N. (1994). Soot formation in partially diffusion flames at atmospheric pressure, In Bockhorn, H. (Ed.) *Soot Formation in Combustion-Mechanism and Models*, Springer-Verlag Berlin, Heidelberg.

Mitchell, P. and Frenklach, M. (2003) Particle aggregation with simultaneous surface growth. *Phys. Rev. E*, **67**(6), Art. No. 061407 Part 1.

Pitsch, H., Chen, M., and Peters, N. (1998) Unsteady flamelet modeling of turbulent hydrogen-air diffusion flames. *Proc. Combust. Instit.*, **27**, 1057–1064.

Pitsch, H. and Peters, N. (1998) A consistent flamelet formulation for non-premixed combustion considering differential diffusion effects. *Combust. Flame*, **114**, 26–40.

Pitsch, H., Riesmeier, E., and Peters, N. (2000) Unsteady flamelet modeling of soot formation in turbulent diffusion flames. *Combust. Sci. Tech.*, **158**, 389–406.

Schuetz, C.A. and Frenklach, M. (2002) Nucleation of soot: molecular dynamics simulations of pyrene dimerization. *Proc. Combust. Instit.*, **29**, 2307–2314.

Young, K.J., Steward, C.D., Syed, K.J., and Moss, J.B. (1991) Soot formation in confined turbulent flames fuelled by pre-vaporised kerosene and by ethylene. *Proc. 10th ISABE Meeting*, AIAA, 239–248.